Frontiers in Bioscience Landmark

Front. Biosci. (Landmark Ed) **2026**; 31(9): 54346
https://doi.org/10.31083/FBL54346

Original Research

Targeting Reductive Stress With Oxygen Enrichment Rescues Hippocampus-Dependent Memory Impairment after Acute Hypobaric Hypoxia

Jiaojiao Ma[1,2,†], Miao Miao[3,†], Xiaohong Liu[1], Xiaohong Tian[1], Chenxu Zhang[1], Yuanzhe Li[1], Chengcheng Zhao[1], Juan Liu[1], Kangning Xie[1], Chi Tang[1,4], Mingming Zhai[1,4,*]

[1]School of Biomedical Engineering, The Air Force Military Medical University, 710032 Xi'an, Shaanxi, China
[2]School of Medicine, Xiamen University, 361102 Xiamen, Fujian, China
[3]Affiliated Hospital of Medical School, Jinling Hospital, Nanjing University, 210093 Nanjing, Jiangsu, China
[4]Shaanxi Provincial Key Laboratory of Bioelectromagnetic Detection and Intelligent Perception, 710032 Xi'an, Shaanxi, China
*Correspondence: zhaimingming@fmmu.edu.cn (Mingming Zhai)
[†]These authors contributed equally.
Academic Editor: Thomas Heinbockel
Submitted: 29 May 2026 Revised: 29 July 2026 Accepted: 7 August 2026 Published: 17 September 2026

Abstract

Background: High-altitude hypobaric hypoxia is known to impair cognitive function, but the underlying mechanistic role of impaired redox homeostasis in this context remains incompletely understood. This study investigated whether acute hypobaric hypoxia induces oxidative stress and redox dysregulation in the hippocampus, and whether oxygen enrichment can mitigate these impairments by restoring redox homeostasis. **Methods:** Spatial memory was assessed using the Morris water maze. Additionally, hippocampal morphology, redox status (including glutathione/oxidized glutathione [GSH/GSSG], the reduced nicotinamide adenine dinucleotide/oxidized nicotinamide adenine dinucleotide [NADH/NAD+], and the reduced nicotinamide adenine dinucleotide phosphate/oxidized nicotinamide adenine dinucleotide phosphate [NADPH/NADP+] ratios, as well as antioxidant enzyme activity levels), and associated molecular pathways were analyzed. **Results:** Following 3 days of hypoxia exposure, rats exhibited impaired spatial memory retention, increased neuronal apoptosis, and reduced neuronal viability in the hippocampal cornu ammonis 1 [CA1] region. The hippocampus displayed significantly altered redox status, characterized by elevated GSH/GSSG, NADH/NAD+, and NADPH/NADP+ ratios, upregulated antioxidant enzymes (superoxide dismutase [SOD], catalase [CAT], and glutathione peroxidase [GPX]), and decreased superoxide levels. These changes are consistent with an adaptive nuclear factor erythroid 2-related factor 2 (Nrf2)-mediated antioxidant response and a shift toward a reductive state. Notably, oxygen enrichment rescued cognitive deficits, attenuated neuronal apoptosis, and normalized redox ratios and the microtubule-associated protein 1A/1B-light chain 3-II/microtubule-associated protein 1A/1B-light chain 3-I (LC3B-II/ LC3B-I) ratio. **Conclusions:** Hypoxia-induced redox dysregulation is closely associated with cognitive impairment. Oxygen enrichment alleviates these deficits by modulating the Nrf2-mediated adaptive response and restoring redox homeostasis, thereby supporting further investigation of oxygen enrichment as a potential neuroprotective strategy.

Keywords: hypobaric hypoxia; oxygen enrichment; redox homeostasis; hippocampus; spatial memory; Nrf2

1. Introduction

Altitudes exceeding 2500 m are classified as high-altitude regions [1]. These environments are characterized by hypobaric conditions, where the lower partial pressure of oxygen results in a drop in the effective oxygen content available to the human body [2]. Rapid ascent to such altitudes can precipitate acute mountain sickness, manifesting as nausea, insomnia, dyspnea, and fatigue [3].

High-altitude cerebral edema (HACE) is a severe neurological sequela triggered by hypobaric hypoxia that is characterized by vasogenic edema and central nervous system dysfunction. Its pathogenesis is primarily attributed to the activation of inflammatory cascades and blood-brain barrier (BBB) disruption, resulting in neuronal injury and synaptic dysfunction [4]. Due to its high metabolic demand and abundance of polyunsaturated fatty acids, the brain is exceptionally susceptible to hypoxic insults, with the hippocampus exhibiting particularly high levels of sensitivity [5,6]. A growing body of evidence suggests that hypobaric hypoxia compromises cognitive functions, including learning and memory. The hippocampal cornu ammonis 1 (CA1) region has been noted as a critical locus for hypoxia-induced damage, exhibiting greater sensitivity compared to other subregions [7,8,9]. There is thus a pressing need to elucidate protective mechanisms for CA1 neurons to inform the development of therapeutic strategies against hypoxia-induced cognitive impairment [10].

Phospholipids, including phosphatidylcholine (PC), phosphatidylserine (PS), and phosphatidylethanolamine

(PE), constitute the structural foundation of neuronal membranes and are integral to the maintenance of membrane fluidity, receptor localization, synaptic plasticity, and autophagosome biogenesis. Studies utilizing 31P-magnetic resonance spectroscopy (31P-MRS) combined with metabolomics approaches have uncovered a positive correlation between cerebral phospholipid metabolic indices and performance in memory and executive function tasks [11]. In animal models, acute hypobaric hypoxia exposure at 6700 meters precipitates a decline in choline levels and triggers impaired phospholipid biosynthesis [12,13]. Human metabolomic profiling has further revealed that high-altitude exposure significantly modulates glycerophospholipid pathways, with this metabolic shift coinciding with the onset of cognitive deterioration [14]. These metabolic perturbations likely interact with altitude-induced cerebral edema and redox imbalance, leading to the broader exacerbation of cognitive deficits.

Redox homeostasis is fundamental to cellular physiology. While oxidative stress has been extensively characterized in the context of high-altitude hypoxia, the pathological implications of the opposing extreme—an excessive shift toward a reduced state, termed reductive stress—remain poorly understood [15]. Studies published to date have largely focused on the deleterious effects of oxidative stress on the nervous system under hypobaric hypoxia [16,17]. The nuclear factor erythroid 2-related factor 2 (Nrf2) signaling pathway functions as a primary defense mechanism upon hypoxia exposure, with nuclear Nrf2 translocation triggering the upregulation of antioxidant gene expression and the restoration of redox balance. However, excessive or prolonged activation of this adaptive response, when combined with the hypoxia-induced accumulation of reducing equivalents (e.g., reduced nicotinamide adenine dinucleotide [NADH] and reduced nicotinamide adenine dinucleotide phosphate [NADPH]) due to electron transport chain inhibition, may disrupt redox homeostasis and favor a hyper-reduced cellular state [18,19]. Although evidence suggests that such a reductive shift may impair synaptic function and contribute to cognitive decline [20], it may also represent a maladaptive consequence of the physiological attempt to counteract hypoxia. Consequently, indiscriminate enhancement of antioxidant capacity may not be universally beneficial and theoretically has the potential to exacerbate this reductive shift if redox homeostasis is not strictly regulated [21,22,23].

Oxygen enrichment has been identified as an effective means of mitigating oxidative damage [24]. In high-altitude plateau environments, each 1% increment in oxygen concentration reduces the physiological equivalent altitude by approximately 300 meters [25]. Empirical evidence indicates that increasing indoor oxygen concentrations by 6% at an altitude of 5000 meters significantly enhances reaction time, hand-eye coordination, and overall cognitive performance [26]. Similarly, in patients with chronic obstructive pulmonary disease (COPD), inhaling oxygen-enriched air improves cerebral and muscular oxygen delivery, thereby augmenting both cognitive and motor functions [27]. Despite these findings, the precise molecular mechanisms by which oxygen enrichment ameliorates cognitive impairment remain elusive, largely due to the paucity of targeted investigations.

The primary objective of this study was to evaluate the efficacy of oxygen enrichment as a means of alleviating cognitive impairment induced by acute hypobaric hypoxia, with a specific focus on spatial memory retention deficits. We further investigated whether oxygen enrichment ameliorates these cognitive deficits by modulating redox status and preventing the pathological accumulation of reducing equivalents, thereby restoring redox homeostasis. Specifically, we analyzed whether observed alterations in antioxidant markers and redox ratios align with a shift toward a reductive state, and clarified how oxygen enrichment modulates this metabolic trajectory to preserve hippocampal function.

2. Materials and Methods

2.1 Animals and Experimental Design

Eighteen male Sprague-Dawley rats (7 weeks old) were obtained from the Animal Center of the Air Force Military Medical University. The experimental protocol was approved by the Institutional Animal Care and Use Committee of the The Air Force Military Medical University (20260073), and all procedures were conducted in strict accordance with the National Institutes of Health Guide for the Care and Use of Laboratory Animals. Rats were housed under controlled environmental conditions: temperature (23 °C ± 1 °C), relative humidity (40%–60%), and a 12-hour light/dark cycle.

Rats were randomized into three groups (n = 6): the Normal Control group (NN), the Hypobaric Hypoxia group (HH), and the Hypobaric Oxygen-enrichment group (HO). The sample size for each group (n = 6) was determined based on prior studies from our laboratory, which have proven sufficient to detect significant differences. Rats in the NN group were housed in a normoxic environment in Xi'an (400 m above sea level). Rats in the HH and HO groups were exposed to simulated high-altitude hypobaric hypoxia (equivalent to 7000 m) in a hypobaric chamber (ProOx810L; Tow Tech, Shanghai, China) for 3 days.

The HO group received oxygen enrichment via a custom-developed device designed to simulate the oxygen therapy provided to high-altitude residents while sleeping. To account for the reversed circadian rhythms of rats compared to humans, oxygen was administered for 12 hours per day during their rest phase (08:00–20:00) [28]. The oxygen enrichment system, comprising a portable oxygen concentrator and an individually ventilated cage (IVC), was placed inside the hypobaric chamber to create a localized oxygen-enriched microenvironment within the hy-

poxic atmosphere. Environmental conditions (temperature and housing) within the device were consistent with those of the NN and HH groups. To minimize experimental variability caused by chamber opening, sufficient food and water were provided to ensure ad libitum access throughout the modeling period [29]. Preliminary measurements using an oxygen analyzer (OXYMAT61; Siemens, Erlangen, Germany) confirmed that the oxygen concentration within the IVC remained stable at 28.0% ± 0.2%.

2.2 Sample Collection

At the designated time points, rats were euthanized with 1% sodium pentobarbital (50 mg/kg, Sigma-Aldrich, St. Louis, MO, USA), and hippocampal tissues were rapidly dissected. Samples were immediately snap-frozen and stored at −80 °C until further analysis.

2.3 Morris Water Maze

The Morris water maze (MWM) was employed to evaluate spatial memory retention. To ensure objectivity, all behavioral tests and subsequent data analyses were performed by an investigator blinded to the experimental group assignments. Video recordings were randomly coded and decoded only after the analysis had been completed. The protocol consisted of a 5-day acquisition phase, followed by a probe trial on Day 9 (post-intervention). The entire MWM procedure was conducted under normobaric normoxic conditions.

During the acquisition phase, rats underwent four training trials each day. For every trial, rats were released from one of four different quadrants, with the platform position remaining fixed throughout this phase. The latency for rats to reach the platform within a 120 s time limit was recorded. If a rat failed to locate the platform by this time limit, it was gently guided to the platform and allowed to remain there for 15 s. Training sessions were conducted at consistent times each day, and the swimming path and escape latency were documented.

After completing the acquisition phase, rats in each group were exposed to 3 days of hypobaric hypoxia or oxygen-enriched conditions. Following the exposure, a probe trial was conducted. In this trial, the platform was removed, and rats were randomly placed in different quadrants to swim for 120 s. The following parameters were recorded: the number of platform crossings, the number of times the rats entered the target quadrant, and the duration spent in the target quadrant. These measures were used to assess spatial memory retention.

2.4 Histomorphologic Analyses

2.4.1 Hematoxylin-Eosin (H&E) Staining

After the modeling phase, rats were euthanized with a 1% sodium pentobarbital solution (50 mg/kg). The excised brain tissue was first fixed in 4% paraformaldehyde (P0099, Beyotime, Shanghai, China), then embedded in paraffin wax, and sectioned using standard pathological techniques.

Coronal sections (5 µm thick) of paraffin-embedded whole rat brains were deparaffinized in xylene and rehydrated through a graded ethanol series. The sections were stained with hematoxylin, differentiated with 1% acid-alcohol, blued, and then counterstained with eosin. Subsequently, the sections were dehydrated through a graded ethanol series, cleared in xylene, and mounted with neutral resin. The hippocampal CA1 region was scanned using an Olympus VS200 digital slide microscope (Olympus Corporation, Tokyo, Japan). Histological counting was performed by an independent researcher blinded to the treatment groups. The digital slide images were anonymized and randomly numbered before microscopic examination to maintain blinding. Under blinded conditions, five random fields were selected, and the number of normal neurons per unit area was quantified using the Fiji software (version 1.54f, National Institutes of Health, Bethesda, MD, USA).

2.4.2 Terminal deoxynucleotidyl transferase dUTP nick end labeling (TUNEL) Staining

For terminal deoxynucleotidyl transferase dUTP nick end labeling (TUNEL) staining, paraffin-embedded sections were deparaffinized and rehydrated using the same approach outlined for hematoxylin and eosin (H&E) staining. The sections were treated with proteinase K for permeabilization, and TUNEL staining was then performed using a commercial kit (GB1501, Service Bio, Wuhan, Hubei, China) in strict accordance with the manufacturer's instructions. After washing with phosphate-buffered saline (PBS)(G4202, ServiceBio, Wuhan, Hubei, China), the sections were blocked with 5% bovine serum albumin (BSA) for 30 min at room temperature, followed by incubation with a rabbit anti-NeuN primary antibody (1:3000, GB11138, Service Bio) overnight at 4 °C. Sections were then incubated with a Cy3-conjugated goat anti-rabbit secondary antibody (1:300, GB21303, Service Bio) for 1 h at room temperature in the dark, and nuclei were counterstained with 4′,6-diamidino-2-phenylindole (DAPI). To avoid observer bias, all fluorescence images were acquired, and the TUNEL-positive cells were quantified by an investigator blinded to the experimental group allocation. Finally, images were captured using an Olympus FV31S fluorescence microscope (Olympus, Tokyo, Japan).

2.5 Superoxide Anion Quantification

Superoxide anion generation in rat hippocampal neuronal cells was quantified via superoxide fluorescence staining. Tissue boundaries were delineated with a histochemical pen, and an autofluorescence quencher was applied for 5 minutes. The sections were then incubated with superoxide staining solution (D7008, Sigma-Aldrich, St. Louis, MO, USA) for 30 minutes. After incubation, slides were washed with PBS and counterstained with DAPI for 10 minutes at room temperature, followed by three additional PBS washes and mounting with an anti-fade medium.

Superoxide-positive cells were visualized using a fluorescence microscope (FV31S, Olympus, Japan). While dihydroethidium (DHE) is widely used as a selective probe for superoxide, it is not DHE-specific and may also interact with other reactive oxygen species (ROS). Thus, the fluorescence signal from these analyses should be interpreted as a primary indicator of superoxide levels with this technical limitation in mind.

2.6 Redox-Related Marker and Enzyme Analyses

Superoxide dismutase (SOD) (A001-1, Nanjing Jiancheng Bioengineering Institute, Nanjing, Jiangsu, China), glutathione peroxidase (GPX) (G4307, Servicebio, China), catalase (CAT) (S0051, Beyotime, China), and the levels of reduced/oxidized glutathione (GSH/GSSG) (S0053, Beyotime, China), nicotinamide adenine dinucleotide (NADH/NAD+) (S0175, Beyotime, China), and nicotinamide adenine dinucleotide phosphate (NADPH/NADP+) (S0180S, Beyotime, China) were measured using appropriate commercial kits.

2.7 RNA-Seq

Hippocampal tissues from the NN, HH, and HO groups were collected, with three replicates per group. The samples were sequenced by Gene Denovo Biotechnology (Guangzhou, Guangdong, China), and the sequencing results were analyzed using Omicsmart (Gene Denovo, Guangzhou, Guangdong, China). Differentially expressed genes (DEGs) were identified based on the following criteria: $|\log2FC| > 1.5$ and $p < 0.05$.

2.8 Quantitative RT-qPCR

Total RNA was extracted from hippocampal tissues using the TRIzol reagent (15596018CN, Invitrogen, Carlsbad, CA, USA). The purified RNA was then reverse-transcribed into cDNA using the PrimeScript™ RT reagent Kit (RR036A, Takara, Shiga, Japan). Quantitative real-time PCR (RT-qPCR) was performed on a Roche LightCycler® 480 System using TB Green® Premix Ex Taq™ (RR820A, Takara, Shiga, Japan). Target gene expression levels were normalized to *β-actin* and quantified using the $2^{-\Delta\Delta Ct}$ method. All primer sequences are listed in **Supplementary Table 1**.

2.9 Enzyme-Linked Immunosorbent Assays

PS (MM-70763R2, Meimian, Yancheng, Jiangsu, China), PC (MM-71548R2, Meimian, China), and PE (MM-71078R2, Meimian, China) contents were measured with appropriate commercial enzyme-linked immunosorbent assay (ELISA) kits used in accordance with the manufacturer's instructions.

2.10 Transmission Electron Microscopy

The ultrastructural characteristics of autophagosomes and mitochondria were examined using transmission electron microscopy (TEM; HT7800/HT7700, Hitachi High-Tech Corporation, Tokyo, Japan). Following cerebral perfusion with normal saline and fixation with a mixture of 4% paraformaldehyde and 2.5% glutaraldehyde, hippocampal tissue blocks (1 mm^3) were post-fixed in 1.0% osmium tetroxide, dehydrated, resin-embedded, and polymerized. Ultrathin sections (60 nm) were cut, mounted on copper grids, stained, and observed. To ensure objectivity, image acquisition and quantitative analyses were performed by an investigator blinded to the experimental groups. For each group, at least 20 random fields were analyzed. Autophagosome density was quantified using ImageJ (version 1.54f, National Institutes of Health, Bethesda, MD, USA), while mitochondrial damage was evaluated using a semi-quantitative scoring system (0–2) based on ultrastructural integrity, ranging from intact cristae (score: 0) to severe swelling and disruption (score: 2). A minimum of 20 mitochondria were scored per field to ensure statistical reliability.

2.11 Western Blotting

Total protein was extracted from rat hippocampal tissue samples using radioimmunoprecipitation assay (RIPA) (P0013B, Beyotime, Shanghai, China) lysis buffer. Cytoplasmic and nuclear proteins were separated using a commercial kit (P0027, Beyotime, China), in accordance with the manufacturer's protocol. Protein concentrations were determined using a bicinchoninic acid (BCA) protein assay kit (P0010, Beyotime, China). Proteins were separated via sodium dodecyl sulfate (SDS)-polyacrylamide gel electrophoresis and subsequently transferred onto a polyvinylidene difluoride (PVDF) membrane. Following transfer, the membrane was blocked with 5% nonfat milk powder. Membranes were incubated with primary antibodies specific for P62 (1:1000, ab314504, Abcam), LC3B (1:2000, ab192890, Abcam), Nrf2 (1:1000, ab313825, Abcam), β-actin (1:2000, 4967S, CST, USA), and LaminB (1:10,000, 12987-1-AP, Proteintech, USA) overnight at 4 °C. Membranes were then incubated with a secondary antibody (1:5000, GB23303, Servicebio, China) at room temperature for 1 hour. Protein bands were visualized using a chemiluminescence detection kit and an imaging system. Image analysis and quantification were performed using ImageJ. To ensure objectivity, the quantification of band intensity was performed by an investigator blinded to the experimental groups. The image files were coded prior to analysis using ImageJ.

2.12 Statistical Analysis

Statistical analyses were performed using GraphPad Prism 9.4 (GraphPad Software, San Diego, CA, USA). The Kolmogorov-Smirnov test was used to assess distribution normality, and Levene's test was used to evaluate homogeneity of variance. All data satisfied the assumptions of normality and homogeneity of variance. Differences be-

tween groups were analyzed using one-way analyses of variance (ANOVAs) followed by Bonferroni's post hoc test for multiple comparisons. Data are presented as mean ± standard error of the mean (SEM). The threshold for statistical significance was set at $p < 0.05$. No animals were excluded from the analysis.

3. Results

3.1 Effects of Oxygen Enrichment on Spatial Memory Retention Deficits in Rats Induced by Acute Hypobaric Hypoxia

The MWM procedure used in this study is presented in Fig. 1A. Over the 5-day acquisition phase, the time taken to find the platform declined for rats in all three groups as the number of training days increased, indicating that all groups successfully acquired the spatial task. There were no statistically significant differences in daily escape latency among the groups ($p > 0.05$, Fig. 1B).

During the probe trial on day 9, rats in the HH group crossed the platform significantly fewer times than those in the NN group ($p < 0.01$). Conversely, rats in the HO group exhibited a significantly increased frequency of platform crossings compared to those in the HH group ($p < 0.05$; Fig. 1C). Furthermore, HH group rats entered the target quadrant significantly less frequently and spent significantly less time in it compared to NN group rats ($p < 0.001$ and $p < 0.01$, respectively). In contrast, the HO group exhibited a significantly higher frequency of target quadrant entry and spent more time in it than the HH group ($p < 0.05$ for both; Fig. 1D,E). There was no significant difference between the HO and NN groups. Representative path maps from the probe trial are shown in Fig. 1F.

These results demonstrate that oxygen enrichment intervention can ameliorate spatial memory retention deficits induced by acute hypobaric hypoxia in rats.

3.2 Effect of Oxygen Enrichment on Morphological Changes of Neurons in the Hippocampal CA1 Region Under Acute Hypobaric Hypoxia

H&E staining and TUNEL immunofluorescence double-staining approaches were used to examine the morphological impact of oxygen enrichment (Fig. 2). After 3 days of acute hypobaric hypoxia exposure, the nuclei of neurons in the CA1 region of the hippocampus in the HH group exhibited shrinkage, together with a more chaotic neuronal distribution and a decrease in the number of neurons per unit area. In contrast, the number of neurons per unit area in the HO group was significantly increased ($p < 0.05$), and the neurons in this group were more tightly arranged (Fig. 2A,B). Additionally, fluorescence staining revealed a marked increase in the proportion of neuronal apoptosis in the HH group compared to the NN group ($p < 0.001$), whereas the proportion of neuronal apoptosis in the HO group was lower than that in the HH group ($p < 0.05$, Fig. 2C,D). These findings suggest that oxygen enrichment can mitigate acute hypobaric hypoxia-induced neuronal damage in the rat hippocampus through a reduction in the extent of neuronal apoptosis.

3.3 Effect of Oxygen Enrichment on the Hippocampal Redox State in Acute Hypobaric Hypoxia Model Rats

To investigate the impact of oxygen enrichment on the hypoxia-induced redox imbalance, we conducted superoxide staining on rat hippocampal tissues and assessed corresponding redox indicators (Fig. 3).

Superoxide fluorescence staining revealed a significant decrease in hippocampal superoxide content in rats from the HH group compared to the NN group ($p < 0.001$). Following oxygen-enrichment, however, superoxide levels increased significantly ($p < 0.01$) compared with the HH group, with no significant difference in these levels between the NN and HO groups (Fig. 3A,B).

To rigorously characterize this altered redox landscape, we measured the ratios of major cellular redox couples. The HH group exhibited significantly elevated GSH/GSSG, NADPH/NADP+, and NADH/NAD+ ratios compared to the NN group ($p < 0.01$; $p < 0.05$; $p < 0.05$, respectively), indicating a profound shift toward a highly reduced intracellular state. Oxygen enrichment intervention significantly reversed these changes, bringing the GSH/GSSG and NADPH/NADP+ ratios back toward the levels observed in control rats from the NN group ($p < 0.001$; $p < 0.01$) (Fig. 3C–E).

Analyses of antioxidant enzymes further revealed significant increases in CAT ($p < 0.01$), GPX ($p < 0.01$), and SOD ($p < 0.05$) levels in the HH group compared to the NN group. Oxygen enrichment significantly mitigated these increases (CAT, $p < 0.0001$; GPX, $p < 0.01$; SOD, $p < 0.01$), restoring enzyme expression to levels comparable to those in the NN group (Fig. 3F–H).

Collectively, this convergence of decreased superoxide levels, the accumulation of reducing equivalents (NADH/NADPH), and antioxidant enzyme overactivation strongly suggests that acute hypobaric hypoxia induces a state of reductive stress. Oxygen enrichment effectively alleviates this redox dysregulation, thereby helping to restore physiological redox homeostasis.

3.4 Transcriptomic Sequencing Analysis of Rat Hippocampal Tissue

RNA-Seq was next used to analyze samples from the NN, HH, and HO groups to identify potential molecular targets associated with the ability of oxygen enrichment to protect against hypoxia-induced cognitive impairment. Principal component analysis (PCA) was performed to assess repeatability between samples. The scattered points corresponding to the NN, HH, and HO samples exhibited mutual aggregation within each group and clear differentiation among groups, indicating relatively good intra-group repeatability and high similarity among the sample data (Fig.

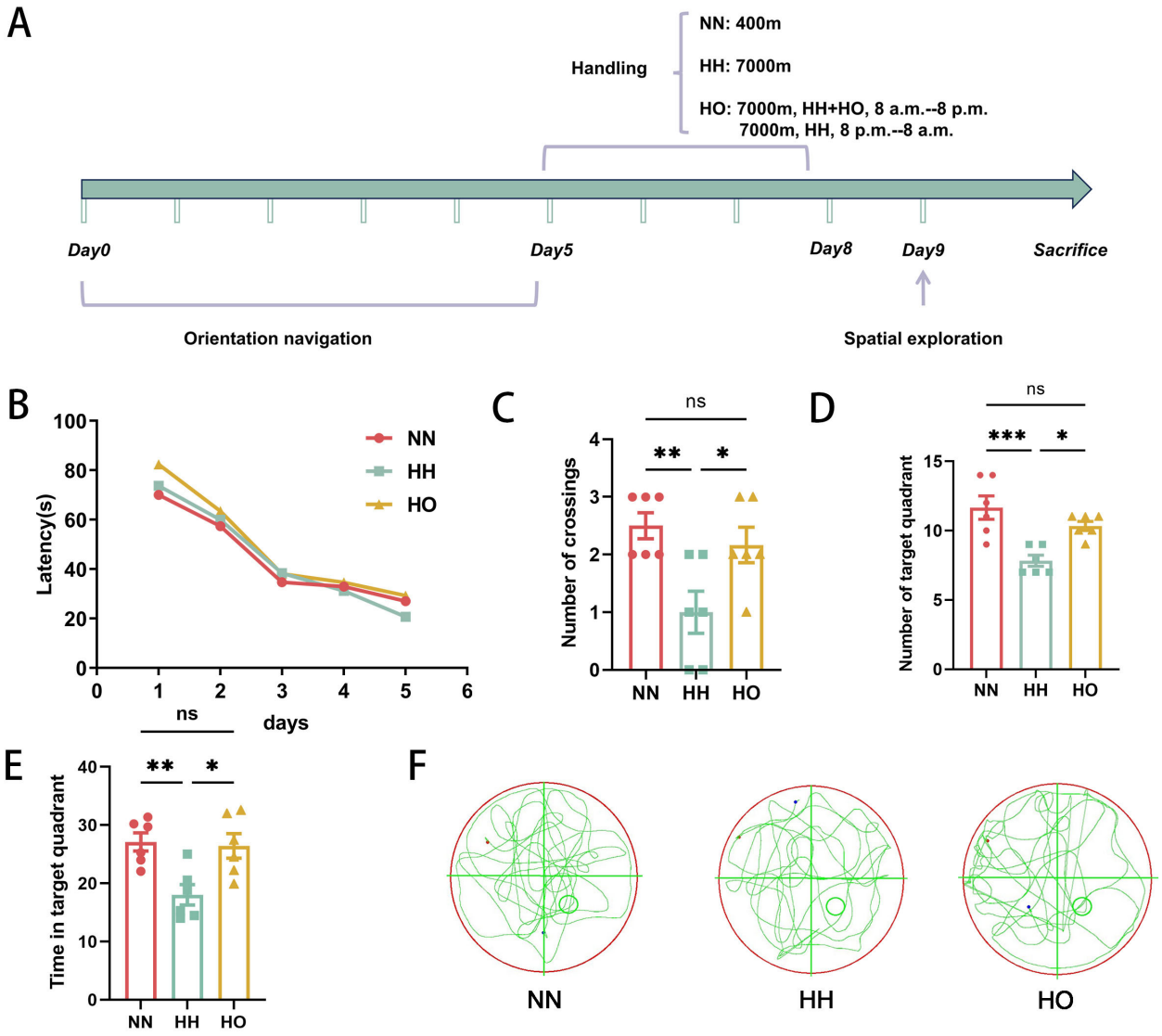

Fig. 1. Effects of oxygen enrichment on spatial memory retention in the Morris water maze test. (A) Schematic timeline of the Morris water maze experiment. (B) Escape latency values for rats in the three study groups during the acquisition phase. (C–E) Quantification of the number of platform crossings, the frequency of target quadrant entry, and the duration spent in the target quadrant during the probe trial. (F) Representative swimming paths during the probe trial. All data are presented as mean ± S.E.M. (n = 6, *p < 0.05, **p < 0.01, ***p < 0.001, ns, no statistically significant difference ($p \geq 0.05$)). NN, Normal Control group; HH, Hypobaric Hypoxia group; HO, Hypobaric Oxygen-enrichment group.

4A). A total of 412 up-regulated and 212 down-regulated genes were identified in the HH group compared with the NN group (Fig. 4B), while 138 up-regulated and 172 down-regulated genes were identified in the HO group compared with the HH group (Fig. 4C). In total, 99 overlapping DEGs were identified for the NN vs. HH and HH vs. HO group comparisons (Fig. 4D). Trend analysis of these 99 DEGs revealed that Profile 5 was significant (Fig. 4E). As shown in Fig. 4F, 40 DEGs from Profile 5 were annotated using a Gene Ontology (GO) enrichment analysis approach and categorized into three main modules. In the biological processes module, these DEGs were primarily associated with cellular adhesion, biological regulation, metabolic reactions, signal transduction, and immune system responses. In the molecular function module, these DEGs were predominantly associated withcatalytic activity, regulation of molecular functions, and adenosine triphosphate (ATP)-related activity. With respect to the cellular component module, these DEGs were mainly associated with cellular anatomical entities and protein complexes. The Kyoto Encyclopedia of Genes and Genomes (KEGG) pathway enrichment analysis was additionally conducted on 40 DEGs identified in Profile 5. Among the analyzed pathways, glycerophospholipid metabolism exhibited the most

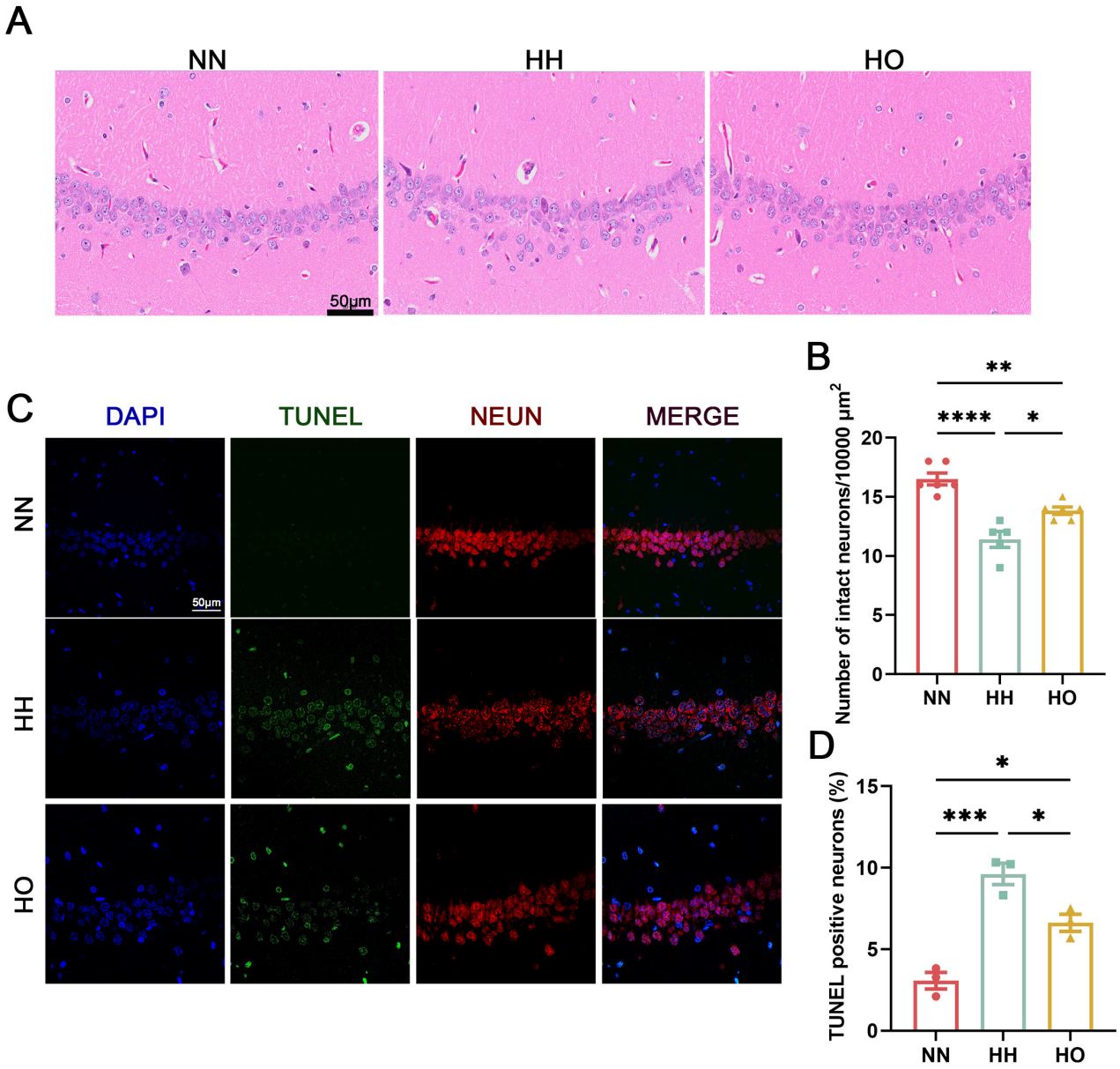

Fig. 2. Morphological assessment of the effects of oxygen enrichment on hippocampal neurons. (A) Representative map of the hippocampal cornu ammonis 1 (CA1) region in rats. (B) Quantification of the number of normal neurons per unit area in the CA1 region of the hippocampus for rats in the indicated groups. (C) Representative terminal deoxynucleotidyl transferase dUTP nick end labeling (TUNEL) staining of hippocampal CA1 samples from rats in the indicated groups. (D) Statistical analysis of TUNEL-positive apoptosis-like neurons in the CA1 region of the hippocampus in rats from the indicated groups. Scale bar = 50 μm. All data are presented as mean ± S.E.M. (n = 3, *$p < 0.05$, **$p < 0.01$, ***$p < 0.001$, ****$p < 0.0001$).

significant enrichment (Fig. 4G). RT-qPCR validation of four representative DEGs (*Etnppl*, *Pla2g3*, *Gpd1*, and *Pnpla7*) revealed expression trends consistent with the RNA-Seq data, confirming the reliability of the sequencing results (Fig. 4H–K). Based on these results and prior research, glycerophospholipid metabolism may be closely associated with the molecular mechanisms by which oxygen enrichment alleviates hypobaric hypoxia-induced spatial learning and memory impairments.

3.5 Effects of Oxygen Enrichment on Hippocampal Glycerophospholipid Metabolism and Autophagy in Acute Hypobaric Hypoxia Model Rats

To investigate the effect of oxygen enrichment on glycerophospholipid metabolic dysregulation in response to acute hypobaric hypoxia, we quantified three phospholipid metabolites in the rat hippocampus via ELISA. Compared to the NN group, the PS, PE, and PC levels in the HH group were significantly reduced ($p < 0.05$, $p < 0.05$, $p < 0.01$).

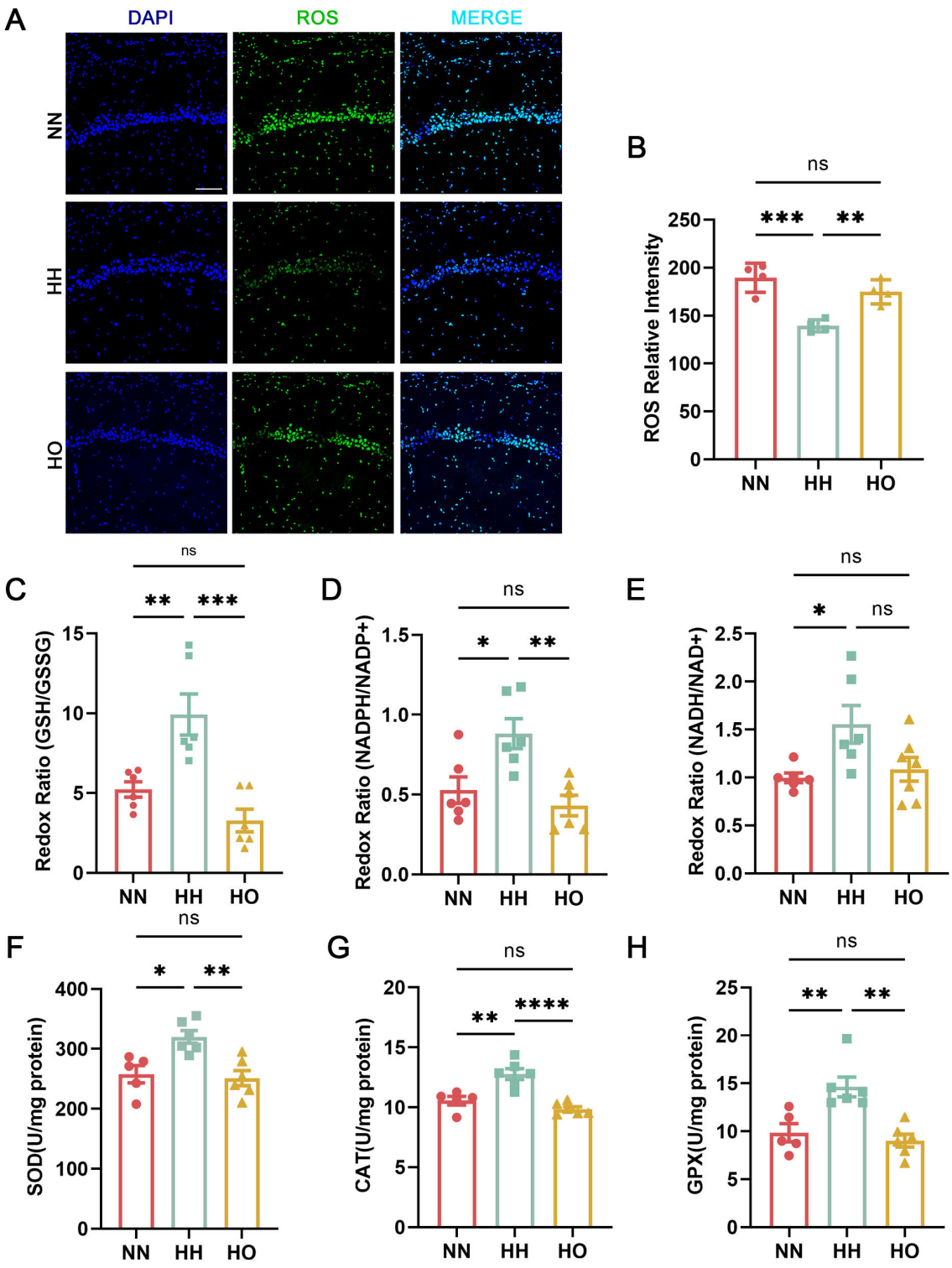

Fig. 3. Evaluation of the effect of oxygen enrichment on reductive stress. (A) Representative superoxide staining of the hippocampal CA1 region for rats in the indicated groups. Scale bar = 50 μm. (B) Quantitative analysis of superoxide fluorescence staining in the hippocampal CA1 region from rats in the indicated groups. (C–E) GSH/GSSG, NADPH/NADP+, and NADH/NAD+ ratios in the indicated groups. (F–H) Quantitative analysis of SOD, CAT, and GPX levels in the indicated groups. All data are presented as mean ± S.E.M. (n = 6, *$p < 0.05$, **$p < 0.01$, ***$p < 0.001$, ****$p < 0.0001$, ns, no statistically significant difference ($p \geq 0.05$)). SOD, Superoxide dismutase; CAT, catalase; GPX, glutathione peroxidase; GSH/GSSG, glutathione/oxidized glutathione; NADH/NAD+, reduced nicotinamide adenine dinucleotide/oxidized nicotinamide adenine dinucleotide; NADPH/NADP+, reduced nicotinamide adenine dinucleotide phosphate/oxidized nicotinamide adenine dinucleotide phosphate.

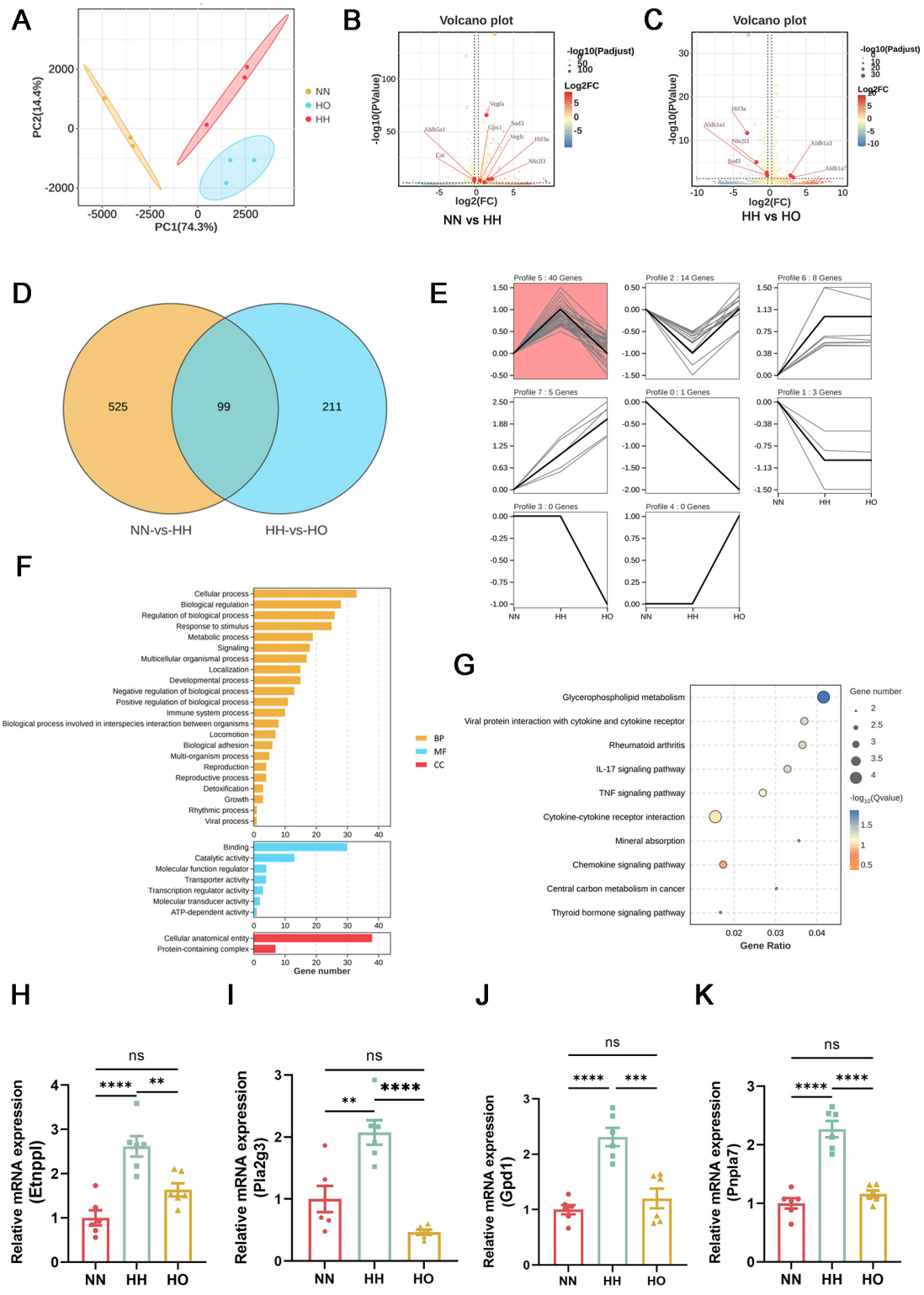

Fig. 4. Transcriptomic sequencing analyses of rat hippocampal tissue. (A) Principal component analysis of reproducibility among samples. (B) Differentially expressed genes (DEGs) identified when comparing the NN and HH groups. (C) DEGs identified when comparing the HH and HO groups. (D) Venn diagram of DEGs identified between the NN and HH groups and between the HH and HO groups. (E) Trend analysis of 99 DEGs. (F) Gene Ontology (GO) enrichment analysis of DEGs in Profile 5. (G) Kyoto Encyclopedia of Genes and Genomes (KEGG) pathway analysis of DEGs in Profile 5. (H–K) Quantitative real-time PCR (RT-qPCR) verification of RNA-seq results. All data are presented as mean ± S.E.M. (For A–G, n = 3, for H–K, n = 6, $^{**}p < 0.01$, $^{***}p < 0.001$, $^{****}p < 0.0001$, ns, no statistically significant difference ($p \geq 0.05$)).

Following oxygen enrichment, these levels of PS, PE, and PC were notably increased ($p < 0.01$; Fig. 5A–C).

To explore the potential link between autophagy and redox regulation, we assessed autophagy levels by detecting the expression of LC3B II/I and P62. Additionally, we evaluated the nuclear translocation of Nrf2, a key regulator of antioxidant responses, by measuring its expression in both the cytoplasm and nucleus. TEM was additionally used to observe autophagosomes and mitochondria.

TEM analysis indicated that mitochondria in the HH group harbored swollen and fractured cristae, contrasting with the intact structures observed in the NN group (Fig. 5D). Mitochondrial damage scores were significantly higher in the HH group (Fig. 5F, $p < 0.05$). Oxygen enrichment alleviated cristae swelling and fracturing, with damage scores showing a downward trend, albeit one that did not achieve statistical significance (Fig. 5F, $p > 0.05$). When evaluating autophagy, the HH group displayed markedly reduced autophagosome formation, consisting mostly of mature structures lacking early-stage forms or fusion intermediates. Autophagosome density was significantly reduced compared to the NN group (Fig. 5E, $p < 0.05$). Oxygen enrichment restored autophagosome formation in treated rats, with numerous early-stage and fusion structures observed, corresponding to a notable albeit non-significant increase in autophagosome numbers (Fig. 5E, $p > 0.05$).

Western blotting showed (Fig. 5I) that acute hypobaric hypoxia exposure led to decreased expression of LC3B II/I ($p < 0.05$, Fig. 5G) and increased P62 expression ($p < 0.05$, Fig. 5H). Conversely, oxygen-enriched intervention increased LC3B II/I expression ($p < 0.05$, Fig. 5G) and decreased P62 expression ($p < 0.05$, Fig. 5H). Hypobaric hypoxia also resulted in elevated Nrf2 expression in the nucleus ($p < 0.01$, Fig. 5K), whereas oxygen enrichment reversed this nuclear Nrf2 expression ($p < 0.05$, Fig. 5K). Cytoplasmic Nrf2 levels did not differ significantly among the NN, HH, and HO groups (Fig. 5J).

These results indicate that hypobaric hypoxia leads to the dysregulation of glycerophospholipid metabolism in the rat hippocampus, accompanied by significant nuclear Nrf2 translocation. Oxygen enrichment can reverse these metabolic abnormalities, reestablish the dynamic phospholipid metabolism balance within the brain, modulate the Nrf2-mediated adaptive response, stabilize redox homeostasis, and improve spatial memory retention impairment in rats exposed to hypobaric hypoxia.

4. Discussion

In our previous work, we established a hypobaric oxygen enrichment system and observed its potential efficacy as a means of ameliorating spatial memory retention deficits in rats under hypobaric hypoxia conditions [30]. Building on these results, in the present study we investigated whether these cognitive benefits are linked to the restoration of redox homeostasis. Using a hypobaric hypoxia chamber, we successfully established a model of spatial memory impairment, as evidenced by worsened MWM performance. Crucially, biochemical assessments revealed that this impairment was associated with the pronounced onset of reductive stress, characterized by the overactivation of the antioxidant system (elevated SOD, CAT, GPX) and the accumulation of reducing equivalents (elevated GSH/GSSG, NADPH/NADP+, and NADH/NAD+ ratios). While fluorescence staining revealed a concomitant decrease in superoxide levels, this likely reflects the scavenging activity of the upregulated antioxidant enzymes rather than a lack of redox perturbation. Furthermore, transcriptomic sequencing identified glycerophospholipid metabolism as a key pathway potentially responsive to oxygen enrichment. Collectively, our data suggest that the crosstalk between glycerophospholipid metabolism and autophagy-related markers may be involved in the adaptive response to reductive stress, potentially contributing to the alleviation of spatial memory deficits in this hypobaric hypoxia model.

Redox homeostasis relies on preserving a delicate balance between oxidant levels and antioxidant activity. While oxidative stress is commonly associated with hypoxia [31], excessive activation of the antioxidant system can conversely drive the cellular environment toward a hyper-reduced state, a phenomenon known as reductive stress [32,33]. Under hypoxic conditions, mitochondrial dysfunction often leads to the accumulation of reducing equivalents [34]. Consistent with this, our study observed significantly elevated hippocampal GSH/GSSG, NADH/NAD+, and NADPH/NADP+ ratios in rats exposed to acute hypobaric hypoxia. Crucially, this accumulation of reducing equivalents was accompanied by the marked upregulation of antioxidant enzymes, including SOD, CAT, and GPX. This biochemical profile provides a mechanistic explanation for our DHE staining results, as the significant decrease in superoxide levels may be associated with the high levels of scavenging activity attributable to the overexpressed SOD, rather than a simple reduction in metabolic activity. This state of reductive stress, characterized by depleted superoxide availability and excessive reducing power, can impair neurogenesis and disrupt redox-sensitive signaling pathways essential for synaptic plasticity [35]. Consequently, the spatial memory deficits observed in the MWM test may not be the sole result of oxidative damage, but could potentially be associated with this maladaptive reductive shift that hinders appropriate superoxide-mediated signal transduction. Notably, oxygen enrichment intervention reversed these alterations, normalizing these hippocampal redox ratios and antioxidant enzyme levels while restoring superoxide levels to within the normal physiological range. These findings suggest that oxygen enrichment alleviates memory impairment by rescuing the hippocampus from reductive stress and restoring redox homeostasis.

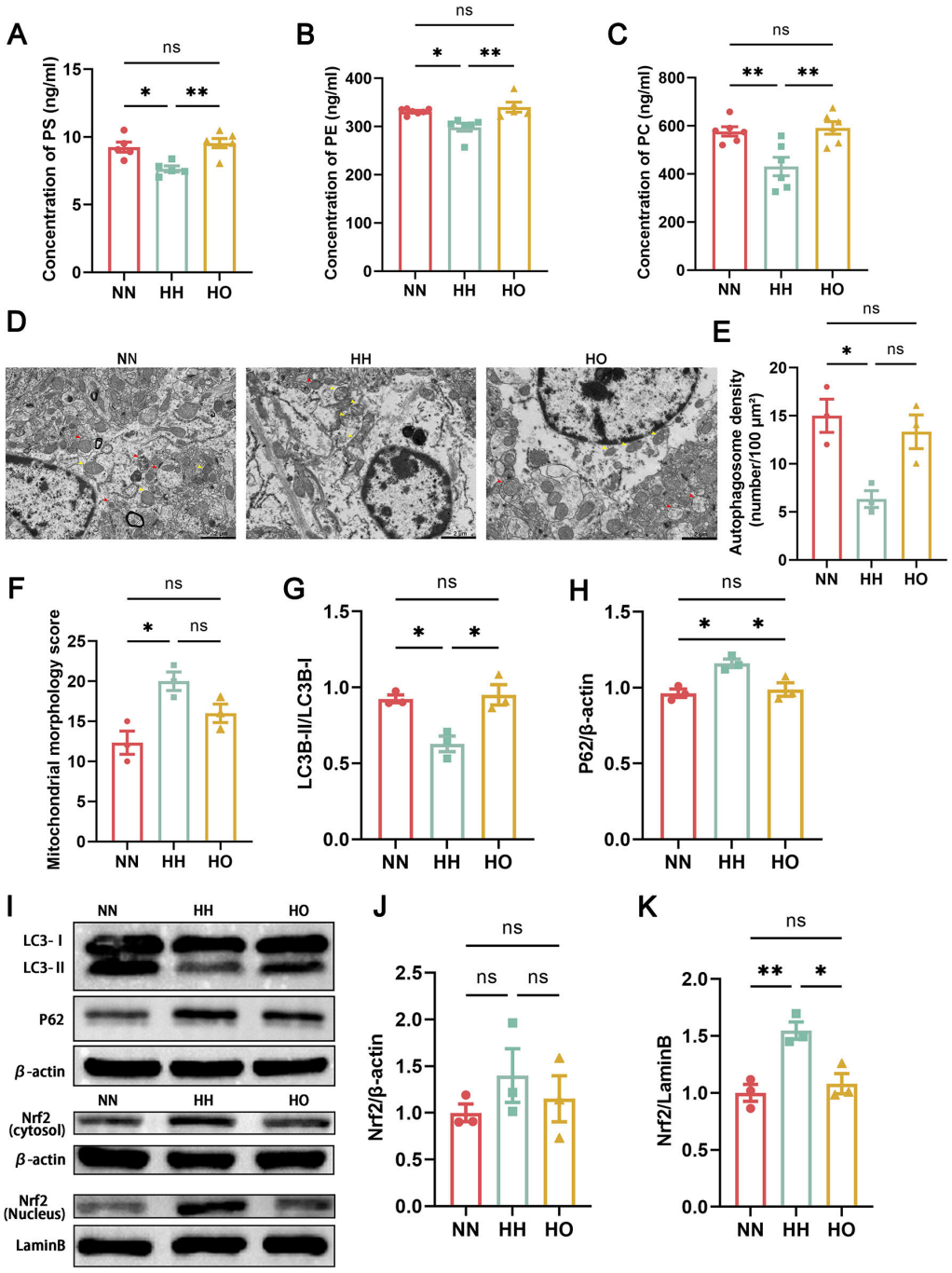

Fig. 5. Effects of oxygen enrichment on hippocampal glycerophospholipid metabolism and autophagy-related markers. (A–C) Content of phospholipid metabolites (PS, PE, PC) in rat hippocampal samples (n = 6). (D) Representative transmission electron microscopy images of mitochondria and autophagosomes in the hippocampal CA1 region. Red arrows indicate autophagosomes, while yellow arrows indicate mitochondria. Scale bar = 2 μm. (E) Quantification of autophagosome density (number/100 μm^2) in the rat hippocampal CA1 region. (F) Mitochondrial morphology scores (0–2) based on ultrastructural integrity, where 0 indicates intact cristae, and 2 indicates severe swelling and disruption. (G,H) Relative LC3B and P62 protein levels. (I) Representative western blotting images of autophagy-related proteins (LC3B and P62) and nuclear/cytoplasmic nuclear factor erythroid 2-related factor 2 (Nrf2) in the rat hippocampus. (J,K) Relative expression of Nrf2 in the cytoplasm and the nucleus. All data are presented as mean ± S.E.M. (n = 3, *$p < 0.05$, **$p < 0.01$, ns, no statistically significant difference ($p \geq 0.05$)). PC, phosphatidylcholine; PS, phosphatidylserine; PE, phosphatidylethanolamine.

To further elucidate the downstream effectors linking redox homeostasis to neuronal function, we performed transcriptomic sequencing, which identified glycerophospholipid metabolism as being significantly altered following oxygen enrichment. We propose that the observed reductive stress induced by acute hypobaric hypoxia may be involved in this metabolic dysregulation. Mechanistically, an excess of reducing equivalents has been shown to inhibit the activity of lysophosphatidic acid acyltransferase (LPAAT), a key enzyme responsible for phospholipid remodeling [36]. Concurrently, hypoxia-induced depletion of ATP and phosphocreatine limits the cytidine diphosphate (CDP)-choline pathway and acyl-CoA supply, while the downregulation of transcription factors such as peroxisome proliferator-activated receptor alpha (PPARα) and carnitine palmitoyltransferase 1 (CPT1) further diminishes the generation of phospholipid precursors [37,38].

This metabolic blockade results in significant disturbances in the synthesis of PS, PE, and PC, which are crucial for the preservation of neuronal membrane integrity and fluidity [39,40,41]. The impaired synthesis of these phospholipids likely contributes to increased membrane rigidity and the disruption of ion channel function, precipitating intracellular Ca^{2+} overload and activating apoptotic signaling pathways, particularly in the hippocampal CA1 region [42]. Consequently, the spatial memory deficits observed in our study may be associated with this redox-metabolic uncoupling. Notably, oxygen enrichment intervention reversed these metabolic disturbances and restored redox balance. These findings suggest that oxygen enrichment may alleviate memory impairment, potentially via normalizing the redox state and alleviating the reductive inhibition of lipid metabolism, ultimately contributing to the preservation of neuronal membrane homeostasis and function.

A critical question arising from these findings is how oxygen enrichment restores redox balance without inducing detrimental oxidative stress. We speculate that under conditions of hypoxia-induced reductive stress, functional stalling of the mitochondrial electron transport chain occurs due to the lack of terminal electron acceptors, leading to the pathological accumulation of reducing equivalents [43,44,45]. Rather than simply contributing to oxidative load, oxygen enrichment relieves this metabolic blockade. By providing adequate oxygen, the electron transport chain resumes normal flux, consuming the excess reducing equivalents and restoring mitochondrial bioenergetics [46]. The normalization of tissue oxygen tension likely further downregulates the compensatory overexpression of antioxidant enzymes (such as SOD) triggered by hypoxia [47]. Consequently, the observed increase in superoxide levels following oxygen intervention is consistent with a restoration of physiological redox signaling, rather than a shift toward pathological oxidative damage. This precise recalibration may be linked to the recovery of redox-sensitive processes, which are essential for the retention of spatial memory.

Exposure to hypoxia triggers a burst of mitochondrial ROS production, particularly from Complex III, thereby stabilizing hypoxia-inducible factor 1-alpha (HIF-1α) and activating adaptive pathways [44]. However, we propose that cellular redox status is not static but rather something that evolves dynamically based on the duration and severity of hypoxic insult. While early or mild hypoxia may elicit oxidative stress, our model of acute hypobaric hypoxia likely represents a more advanced stage of exposure characterized by severe metabolic constraints and electron transport chain congestion. In this state, the pathological accumulation of reducing equivalents, coupled with a compensatory overactivation of antioxidant defenses (evidenced by elevated SOD and GSH/GSSG ratios), shifts the redox balance toward a reductive state. This concept of reductive stress as a distinct pathological entity has gained traction in recent studies of metabolic disorders, where excessive reducing power disrupts cellular homeostasis [48]. Rather than contradicting the classical hypoxic ROS paradigm, our findings instead highlight a stage-specific transition from oxidative signaling to reductive metabolic failure that takes place within the hypoxic hippocampus.

Phospholipids are integral to autophagic membrane formation and expansion, with continuous lipid recruitment being essential to this dynamic process [49]. The interconversion of these lipids is tightly regulated, with PS being synthesized in the endoplasmic reticulum, whereas PS is synthesized from PC or PE under the activity of serine exchange enzymes. PS then undergoes transport to mitochondria, where it is decarboxylated to regenerate PE. This mitochondrial PE is critical for autophagy, as it serves as the conjugation partner for LC3B-I to form LC3B-II, a key marker of autophagosome formation. Furthermore, P62 acts as an adaptor, linking LC3B to ubiquitinated substrates for lysosomal degradation [50]. Notably, alterations in membrane lipid composition, such as the loss of phospholipid asymmetry induced by exogenous PE, have been shown to trigger apoptosis and autophagy in cultured cells [51]. In line with these mechanisms, oxygen enrichment in the present study reversed the hypobaric hypoxia-induced reduction in autophagosome numbers and the associated downregulation of autophagy-related proteins. These findings suggest that acute hypobaric hypoxia is associated with the suppression of hippocampal autophagosome formation and impaired autophagy-related marker expression, potentially as a consequence of metabolic constraints.

The suppression of autophagic activity observed in this study appears to contradict the findings of Yan Xue et al. [52], who reported that inhibiting autophagy and thereby preventing Claudin-5 degradation attenuated HACE and preserved blood-brain barrier integrity under hypobaric hypoxia. We attribute this apparent discrepancy primarily to the distinct cellular targets and metabolic requirements involved. While Yan Xue et al. [52] focused on cerebral microvascular endothelial cells, our study centers on

hippocampal neurons, which are exceptionally dependent on access to an adequate energy supply [53] and sufficient membrane lipids [54]. We postulate that, under the specific hypobaric hypoxia conditions employed in our study, the resulting energy crisis and impaired phospholipid metabolism create a restrictive environment that suppresses the autophagic pathway in neurons. Unlike the detrimental hyper-autophagy observed in endothelial cells, the suppression of basal autophagy in neurons compromises cellular homeostasis. This neuronal dysfunction therefore likely contributes to secondary BBB disruption, suggesting that cell-type-specific autophagic responses play complementary roles in the pathology of HACE.

Our study demonstrates that oxygen enrichment intervention (28.0% O_2 at simulated 7000 m altitude) effectively restored the hippocampal levels of the three major phospholipids (PS, PE, and PC). These lipidomic changes coincided with the restoration of autophagosome formation and an elevated LC3B-II/LC3B-I ratio, despite the numerical increase in autophagosomes not reaching statistical significance. Given that phospholipids serve as the structural building blocks for the autophagic isolation membrane, and the covalent conjugation of PE to LC3B-I is a prerequisite for LC3B-II generation [55], these findings point to a metabolic mechanism underlying the therapeutic effect of oxygen. We speculate that oxygen enrichment gives rise to elevated tissue oxygen tension, thereby facilitating the recovery of mitochondrial oxidative phosphorylation and ATP production. This restoration of energy availability reactivates the CDP-choline pathway and PE-synthesizing enzymes, ensuring that sufficient PE substrates are available for LC3B-I lipidation and autophagosome biogenesis. However, we acknowledge that this mechanistic explanation remains hypothetical. As our current assessment relies on static markers, we cannot definitively exclude the possibility that impaired autophagic degradation contributes to the observed LC3B-II accumulation noted in this study. Future studies utilizing lysosomal blockers are warranted to distinguish between enhanced biogenesis and impaired turnover to more rigorously validate associated autophagic flux dynamics.

Autophagy is closely associated with redox homeostasis, functioning as both a survival mechanism and a regulator of cellular redox status through the P62-Kelch-like ECH-associated protein 1 (Keap1)-Nrf2 signaling axis [56,57,58]. When autophagic activity is dysfunctional, the adaptor protein P62 accumulates due to impaired degradation. Both the Keap1-interacting region (KIR) motif of P62 and the Neh2 domain in Nrf2 are capable of binding to Keap1. Consequently, accumulated P62 competes with Nrf2 for Keap1 binding, leading to Nrf2 dissociation, nuclear translocation, and subsequent antioxidant gene activation [19]. While this pathway is adaptive, excessive activation can be indicative of underlying proteostatic stress. Our results show that oxygen enrichment can significantly attenuate the hypoxia-induced accumulation of P62. Correspondingly, while nuclear Nrf2 expression was markedly upregulated under hypobaric hypoxia, it returned to baseline levels following oxygen intervention. This suggests that the excessive Nrf2 activation observed under hypoxic conditions may be attributable to P62 accumulation in the context of impaired autophagy. Oxygen enrichment appears to mitigate this compensatory hyperactivation, which is potentially associated with the restoration of autophagic competence and a reduction in P62 burden, ultimately contributing to the re-establishment of redox homeostasis. We recognize, however, that these conclusions are currently based on observational correlations. Future investigations employing genetic or pharmacological manipulations of the P62-Keap1-Nrf2 axis will be essential to causally validate this pathway and further elucidate the crosstalk between lipid metabolism, autophagy, and oxidative stress in the context of HACE.

5. Limitations

While this study offers several notable findings, there are important limitations to these analyses that should be acknowledged. First, this study did not include a control group exposed to normoxia and oxygen enrichment. This omission was due to our specific focus on evaluating the efficacy of oxygen enrichment as an intervention for hypoxia-induced impairments, prioritizing the comparison between untreated hypoxia and treated hypoxia as a means of directly addressing our central research question. Second, the sample size in our behavioral experiments (n = 6) was relatively modest. While our analyses were nonetheless significant, future studies with larger sample sizes and prospective power calculations are warranted to further validate the robustness of these findings. Third, our current evidence reflects significant associations rather than definitive causality. It remains unclear whether the protective effects of oxygen enrichment on the hippocampus and its associated regulation of metabolism and autophagy are strictly dependent on reductive stress. Future investigations employing genetic or pharmacological manipulations will be essential to directly test these causal relationships and to develop a more comprehensive mechanistic understanding thereof. Finally, although DHE staining is commonly employed to estimate superoxide levels, it lacks absolute specificity. Therefore, our DHE-based results should be interpreted in conjunction with independent biochemical markers, such as the SOD and GSH/GSSG ratio, to more comprehensively evaluate cellular redox status.

6. Conclusions

In conclusion, our results demonstrate that oxygen enrichment helps restore redox homeostasis and modulates the adaptive antioxidant response, thereby improving spatial memory impairments caused by acute hypobaric hypoxia.

These neuroprotective effects may be associated with the interplay between glycerophospholipid metabolism and autophagy.

Availability of Data and Materials

The data generated or analyzed during the current study are available from the online supplemental materials or from the corresponding author upon reasonable request.

Author Contributions

JM: Data curation, Formal analysis, Writing—original draft, Investigation, Methodology, Conceptualization. XL: Investigation, Methodology, Writing—review and editing. MM: Investigation, Writing—review and editing. XT: Investigation, Methodology. CZhang: Data curation, Investigation, Visualization, Writing—review and editing. YL: Investigation, Methodology, Writing—review and editing. CZhao: Investigation, Methodology, Writing—review and editing. JL: Investigation, Methodology, Writing—review and editing. KX: Investigation, Methodology, Writing—review and editing. CT: Resources, Supervision, Validation, Writing—review and editing. MZ: Conceptualization, Resources, Writing—review and editing. All authors contributed to editorial changes in the manuscript. All authors read and approved the final manuscript. All authors have participated sufficiently in the work and agreed to be accountable for all aspects of the work.

Ethics Approval and Consent to Participate

Experimental procedures for the animal study were approved by the Institutional Animal Care and Use Committee of The Air Force Military Medical University (20260073) and strictly performed according to the guidelines of the Care and Use of Laboratory Animals published by the National Institutes of Health. All animal experimental procedures were conducted in accordance with the principles of the 3Rs (Replacement, Reduction, and Refinement), and the study was reported following the ARRIVE guidelines for animal research.

Acknowledgment

We gratefully acknowledge the assistance and instruction from Gene Denovo Biotechnology (Guangzhou, Guangdong, China) for RNA-Seq and data analysis.

Funding

The authors declare that financial support was received for the research, authorship, and/or publication of this article. This work was supported by the Youth Fund of the Shaanxi Province Natural Science Foundation (grant number 2022JQ-827) and the Industry-Education-Research Innovation Fund of Chinese University (grant number 2021JH053).

Conflicts of Interest

The authors declare no conflicts of interest. Gene Denovo Biotechnology (Guangzhou, Guangdong, China) provided technical assistance with RNA sequencing and data analysis only and had no role in the study design, interpretation of the results, preparation of the manuscript, or the decision to submit the manuscript for publication.

Declaration of AI and AI-Assisted Technologies in the Writing Process

During the preparation of this work, the authors used ChatGPT-3.5 in order to check spelling and grammar. After using this tool, the authors reviewed and edited the content as needed and take full responsibility for the content of the publication.

Supplementary Material

Supplementary material associated with this article can be found, in the online version, at https://doi.org/10.31083/FBL54346.

References

[1] Ma J, Wang C, Sun Y, Pang L, Zhu S, Liu Y, et al. Comparative study of oral and intranasal puerarin for prevention of brain injury induced by acute high-altitude hypoxia. International Journal of Pharmaceutics. 2020; 591: 120002. https://doi.org/10.1016/j.ijpharm.2020.120002

[2] Li S, Li S, Guan H, Lu E, Cao D, Zhang Q. Multifaceted therapeutic mechanisms underlying high altitude cerebral edema: a systematic review. Discover Medicine. 2025; 2: 187. https://doi.org/10.1007/s44337-025-00430-6

[3] Wu Y, Zhang C, Chen Y, Luo YJ. Association between acute mountain sickness (AMS) and age: a meta-analysis. Military Medical Research. 2018; 5: 14. https://doi.org/10.1186/s40779-018-0161-x

[4] Gatterer H, Villafuerte FC, Ulrich S, Bhandari SS, Keyes LE, Burtscher M. Altitude illnesses. Nature Reviews. Disease Primers. 2024; 10: 43. https://doi.org/10.1038/s41572-024-00526-w

[5] Jing L, Da Q, Zhang S, Zhang J, Ma H, Luo H. Nitronyl Nitroxide Ameliorates Hypobaric Hypoxia-Induced Cognitive Impairment in Mice by Suppressing the Oxidative Stress, Inflammatory Response and Apoptosis. Neurochemical Research. 2024; 49: 785–799. https://doi.org/10.1007/s11064-023-04080-x

[6] Kumari P, Roy K, Wadhwa M, Chauhan G, Alam S, Kishore K, et al. Fear memory is impaired in hypobaric hypoxia: Role of synaptic plasticity and neuro-modulators in limbic region. Life Sciences. 2020; 254: 117555. https://doi.org/10.1016/j.lfs.2020.117555

[7] Pawar H, Ray K, Kishore K. Cognitive Challenges at High Altitude: Human Responses and Adaptation Strategies. In Srivastava S, Sharma M, Varshney R (eds.) Health and Sustenance in Extreme Environment (pp. 153–177). Springer: Singapore. 2025. https://doi.org/10.1007/978-981-96-8642-1_9

[8] Churilova A, Zachepilo T, Baranova K, Rybnikova E. Differences in the Autophagy Response to Hypoxia in the Hippocampus and Neocortex of Rats. International Journal of Molecular Sciences. 2022; 23: 8002. https://doi.org/10.3390/ijms23148002

[9] Kreisman NR, Soliman S, Gozal D. Regional differences in hypoxic depolarization and swelling in hippocampal slices. Jour-

nal of Neurophysiology. 2000; 83: 1031–1038. https://doi.org/10.1152/jn.2000.83.2.1031

[10] Wang LS, Zhou J, Shao XM, Tang XC. Huperzine A attenuates cognitive deficits and brain injury in neonatal rats after hypoxia-ischemia. Brain Research. 2002; 949: 162–170. https://doi.org/10.1016/s0006-8993(02)02977-3

[11] Das N, Ren J, Spence JS, Rackley A, Chapman SB. Relationship of Parieto-Occipital Brain Energy Phosphate Metabolism and Cognition Using ^{31}P MRS at 7-Tesla in Amnestic Mild Cognitive Impairment. Frontiers in Aging Neuroscience. 2020; 12: 222. https://doi.org/10.3389/fnagi.2020.00222

[12] Norton CE, Weise-Cross L, Ahmadian R, Yan S, Jernigan NL, Paffett ML, et al. Altered Lipid Domains Facilitate Enhanced Pulmonary Vasoconstriction after Chronic Hypoxia. American Journal of Respiratory Cell and Molecular Biology. 2020; 62: 709–718. https://doi.org/10.1165/rcmb.2018-0318OC

[13] Koundal S, Gandhi S, Kaur T, Mazumder A, Khushu S. "Omics" of High Altitude Biology: A Urinary Metabolomics Biomarker Study of Rats Under Hypobaric Hypoxia. Omics : a Journal of Integrative Biology. 2015; 19: 757–765. https://doi.org/10.1089/omi.2015.0155

[14] D'Alessandro A, Nemkov T, Sun K, Liu H, Song A, Monte AA, et al. AltitudeOmics: Red Blood Cell Metabolic Adaptation to High Altitude Hypoxia. Journal of Proteome Research. 2016; 15: 3883–3895. https://doi.org/10.1021/acs.jproteome.6b00733

[15] Mallet RT, Burtscher J, Pialoux V, Pasha Q, Ahmad Y, Millet GP, et al. Molecular Mechanisms of High-Altitude Acclimatization. International Journal of Molecular Sciences. 2023; 24: 1698. https://doi.org/10.3390/ijms24021698

[16] Ikonomidou C, Kaindl AM. Neuronal death and oxidative stress in the developing brain. Antioxidants & Redox Signaling. 2011; 14: 1535–1550. https://doi.org/10.1089/ars.2010.3581

[17] Lloret A, Fuchsberger T, Giraldo E, Vina J. Reductive Stress: A New Concept in Alzheimer's Disease. Current Alzheimer Research. 2016; 13: 206–211. https://doi.org/10.2174/1567205012666150921101430

[18] Bellezza I, Giambanco I, Minelli A, Donato R. Nrf2-Keap1 signaling in oxidative and reductive stress. Biochimica et Biophysica Acta. Molecular Cell Research. 2018; 1865: 721–733. https://doi.org/10.1016/j.bbamcr.2018.02.010

[19] Eskla KL, Vellama H, Tarve L, Eichelmann H, Jagomäe T, Porosk R, et al. Hypothermia Alleviates Reductive Stress, a Root Cause of Ischemia Reperfusion Injury. International Journal of Molecular Sciences. 2022; 23: 10108. https://doi.org/10.3390/ijms231710108

[20] S Narasimhan KK, Devarajan A, Karan G, Sundaram S, Wang Q, van Groen T, et al. Reductive stress promotes protein aggregation and impairs neurogenesis. Redox Biology. 2020; 37: 101739. https://doi.org/10.1016/j.redox.2020.101739

[21] Li X, Zhang J, Liu G, Wu G, Wang R, Zhang J. High altitude hypoxia and oxidative stress: The new hope brought by free radical scavengers. Life Sciences. 2024; 336: 122319. https://doi.org/10.1016/j.lfs.2023.122319

[22] Nieto Estrada VH, Molano Franco D, Medina RD, Gonzalez Garay AG, Martí-Carvajal AJ, Arevalo-Rodriguez I. Interventions for preventing high altitude illness: Part 1. Commonly-used classes of drugs. The Cochrane Database of Systematic Reviews. 2017; 6: CD009761. https://doi.org/10.1002/14651858.CD009761.pub2

[23] Pérez-Torres I, Guarner-Lans V, Rubio-Ruiz ME. Reductive Stress in Inflammation-Associated Diseases and the Pro-Oxidant Effect of Antioxidant Agents. International Journal of Molecular Sciences. 2017; 18: 2098. https://doi.org/10.3390/ijms18102098

[24] Nagatomo F, Fujino H, Kondo H, Ishihara A. Oxygen concentration-dependent oxidative stress levels in rats. Oxidative Medicine and Cellular Longevity. 2012; 2012: 381763. https://doi.org/10.1155/2012/381763

[25] West JB. High-altitude medicine. American Journal of Respiratory and Critical Care Medicine. 2012; 186: 1229–1237. https://doi.org/10.1164/rccm.201207-1323CI

[26] Gerard AB, McElroy MK, Taylor MJ, Grant I, Powell FL, Holverda S, et al. Six percent oxygen enrichment of room air at simulated 5,000 m altitude improves neuropsychological function. High Altitude Medicine & Biology. 2000; 1: 51–61. https://doi.org/10.1089/152702900320685

[27] Maldonado D, González-García M, Barrero M, Jaramillo C, Casas A. Exercise endurance in chronic obstructive pulmonary disease patients at an altitude of 2640 meters breathing air and oxygen (FIO2 28% and 35%): a randomized crossover trial. COPD. 2014; 11: 401–406. https://doi.org/10.3109/15412555.2013.836480

[28] Ma Q, Ma J, Cui J, Zhang C, Li Y, Liu J, et al. Oxygen enrichment protects against intestinal damage and gut microbiota disturbance in rats exposed to acute high-altitude hypoxia. Frontiers in Microbiology. 2023; 14: 1268701. https://doi.org/10.3389/fmicb.2023.1268701

[29] West JB. Oxygen Conditioning at High Altitude. High Altitude Medicine & Biology. 2015; 16: 173–174. https://doi.org/10.1089/ham.2015.29002.jbw

[30] Cai J, Ruan J, Shao X, Ding Y, Xie K, Tang C, et al. Oxygen Enrichment Mitigates High-Altitude Hypoxia-Induced Hippocampal Neurodegeneration and Memory Dysfunction Associated with Attenuated Tau Phosphorylation. High Altitude Medicine & Biology. 2021; 22: 274–284. https://doi.org/10.1089/ham.2020.0218

[31] Huo L, Liu X, Wang H. Leukemia Inhibitory Factor Attenuates Hypoxic-Ischemic White Matter Injury via NLRP3 Inflammasome Activity Suppressing Through the Nrf2/HO-1 Pathway. Frontiers in Bioscience (Landmark edition). 2025; 30: 36630. https://doi.org/10.31083/FBL36630

[32] Xiao W, Loscalzo J. Metabolic Responses to Reductive Stress. Antioxidants & Redox Signaling. 2020; 32: 1330–1347. https://doi.org/10.1089/ars.2019.7803

[33] Olatunji OJ, Chen H, Zhou Y. Lycium chinensis Mill attenuates glutamate induced oxidative toxicity in PC12 cells by increasing antioxidant defense enzymes and down regulating ROS and Ca(2+) generation. Neuroscience Letters. 2016; 616: 111–118. https://doi.org/10.1016/j.neulet.2015.10.070

[34] Oldham WM, Clish CB, Yang Y, Loscalzo J. Hypoxia-Mediated Increases in L-2-hydroxyglutarate Coordinate the Metabolic Response to Reductive Stress. Cell Metabolism. 2015; 22: 291–303. https://doi.org/10.1016/j.cmet.2015.06.021

[35] Manford AG, Rodríguez-Pérez F, Shih KY, Shi Z, Berdan CA, Choe M, et al. A Cellular Mechanism to Detect and Alleviate Reductive Stress. Cell. 2020; 183: 46–61.e21. https://doi.org/10.1016/j.cell.2020.08.034

[36] Wang B, Tontonoz P. Phospholipid Remodeling in Physiology and Disease. Annual Review of Physiology. 2019; 81: 165–188. https://doi.org/10.1146/annurev-physiol-020518-114444

[37] Kious BM, Kondo DG, Renshaw PF. Living High and Feeling Low: Altitude, Suicide, and Depression. Harvard Review of Psychiatry. 2018; 26: 43–56. https://doi.org/10.1097/HRP.0000000000000158

[38] Xu J, Chen WJ, Wang Z, Xin MY, Gao SH, Liu WJ, et al. Profiles of transcriptome and metabolic pathways after hypobaric hypoxia exposure. Proteome Science. 2022; 20: 16. https://doi.org/10.1186/s12953-022-00198-y

[39] van der Veen JN, Kennelly JP, Wan S, Vance JE, Vance DE, Jacobs RL. The critical role of phosphatidylcholine and phosphatidylethanolamine metabolism in health and disease. Biochimica et Biophysica Acta. Biomembranes. 2017; 1859:

1558–1572. https://doi.org/10.1016/j.bbamem.2017.04.006
[40] Afshinnia F, Nair V, Lin J, Rajendiran TM, Soni T, Byun J, et al. Increased lipogenesis and impaired β-oxidation predict type 2 diabetic kidney disease progression in American Indians. JCI Insight. 2019; 4: e130317. https://doi.org/10.1172/jci.insight.130317
[41] Scott-Hewitt N, Perrucci F, Morini R, Erreni M, Mahoney M, Witkowska A, et al. Local externalization of phosphatidylserine mediates developmental synaptic pruning by microglia. The EMBO Journal. 2020; 39: e105380. https://doi.org/10.15252/embj.2020105380
[42] Muthuraju S, Pati S. Effect of hypobaric hypoxia on cognitive functions and potential therapeutic agents. The Malaysian Journal of Medical Sciences : MJMS. 2014; 21: 41–45.
[43] Zorov DB, Juhaszova M, Sollott SJ. Mitochondrial reactive oxygen species (ROS) and ROS-induced ROS release. Physiological Reviews. 2014; 94: 909–950. https://doi.org/10.1152/physrev.00026.2013
[44] Guzy RD, Hoyos B, Robin E, Chen H, Liu L, Mansfield KD, et al. Mitochondrial complex III is required for hypoxia-induced ROS production and cellular oxygen sensing. Cell Metabolism. 2005; 1: 401–408. https://doi.org/10.1016/j.cmet.2005.05.001
[45] Chandel NS, Maltepe E, Goldwasser E, Mathieu CE, Simon MC, Schumacker PT. Mitochondrial reactive oxygen species trigger hypoxia-induced transcription. Proceedings of the National Academy of Sciences of the United States of America. 1998; 95: 11715–11720. https://doi.org/10.1073/pnas.95.20.11715
[46] Tompkins AJ, Burwell LS, Digerness SB, Zaragoza C, Holman WL, Brookes PS. Mitochondrial dysfunction in cardiac ischemia-reperfusion injury: ROS from complex I, without inhibition. Biochimica et Biophysica Acta. 2006; 1762: 223–231. https://doi.org/10.1016/j.bbadis.2005.10.001
[47] Majmundar AJ, Wong WJ, Simon MC. Hypoxia-inducible factors and the response to hypoxic stress. Molecular Cell. 2010; 40: 294–309. https://doi.org/10.1016/j.molcel.2010.09.022
[48] Mladenov M, Sazdova I, Hadzi-Petrushev N, Konakchieva R, Gagov H. The Role of Reductive Stress in the Pathogenesis of Endocrine-Related Metabolic Diseases and Cancer. International Journal of Molecular Sciences. 2025; 26: 1910. https://doi.org/10.3390/ijms26051910
[49] Osawa T, Matoba K, Noda NN. Lipid Transport from Endoplasmic Reticulum to Autophagic Membranes. Cold Spring Harbor Perspectives in Biology. 2022; 14: a041254. https://doi.org/10.1101/cshperspect.a041254
[50] Schütter M, Giavalisco P, Brodesser S, Graef M. Local Fatty Acid Channeling into Phospholipid Synthesis Drives Phagophore Expansion during Autophagy. Cell. 2020; 180: 135–149.e14. https://doi.org/10.1016/j.cell.2019.12.005
[51] Castillo SR, Nguyen MHL, DiPasquale M, Kelley EG, Marquardt D. Mitocans induce lipid flip-flop and permeabilize the membrane to signal apoptosis. Biophysical Journal. 2023; 122: 2353–2366. https://doi.org/10.1016/j.bpj.2023.03.039
[52] Xue Y, Wan B, Wang Z, Wang Z, Wang D, Yang W, et al. Hydroxychloroquine Prevents High-altitude Cerebral Edema by Inhibiting Endothelial Claudin-5 Autophagic Degradation. Current Neuropharmacology. 2026; 24: 404–418. https://doi.org/10.2174/011570159X371235250417051313
[53] Pudelko-Malik N, Drulis-Fajdasz D, Fydryszewski M, Burgess S, Mlynarz P, Rakus D, et al. Glucose-dependent metabolism of hippocampal primary neurons in response to chemically induced long-term potentiation. bioRxiv. 2025. https://doi.org/10.1101/2025.02.24.639988 (preprint)
[54] Wang QS, Yan K, Li KD, Gao LN, Wang X, Liu H, et al. Targeting hippocampal phospholipid and tryptophan metabolism for antidepressant-like effects of albiflorin. Phytomedicine : International Journal of Phytotherapy and Phytopharmacology. 2021; 92: 153735. https://doi.org/10.1016/j.phymed.2021.153735
[55] Chang C, Shi X, Jensen LE, Yokom AL, Fracchiolla D, Martens S, et al. Reconstitution of cargo-induced LC3 lipidation in mammalian selective autophagy. Science Advances. 2021; 7: eabg4922. https://doi.org/10.1126/sciadv.abg4922
[56] Kimmelman AC, White E. Autophagy and Tumor Metabolism. Cell Metabolism. 2017; 25: 1037–1043. https://doi.org/10.1016/j.cmet.2017.04.004
[57] Pal R, Palmieri M, Loehr JA, Li S, Abo-Zahrah R, Monroe TO, et al. Src-dependent impairment of autophagy by oxidative stress in a mouse model of Duchenne muscular dystrophy. Nature Communications. 2014; 5: 4425. https://doi.org/10.1038/ncomms5425
[58] Jiao J, Demontis F. Skeletal muscle autophagy and its role in sarcopenia and organismal aging. Current Opinion in Pharmacology. 2017; 34: 1–6. https://doi.org/10.1016/j.coph.2017.03.009